Available online at www.sciencedirect.com
SCIENCE DIRECT®
Journal of Magnetism and Magnetic Materials 302 (2006) 47–51
www.elsevier.com/locate/jmmm

Magnetic viruses via nano-capsid templates ☆

Chinmei Liu[a], Seok-Hwan Chung[a], Qiaoling Jin[a], April Sutton[a,b], Funing Yan[a,c], Axel Hoffmann[a], Brian K. Kay[a], Samuel D. Bader[a,*], Lee Makowski[a], Liaohai Chen[a,*]

[a]*Biosciences Division, Materials Science Division and Center for Nanoscale Materials, Argonne National Laboratory, Argonne, IL 60439*
[b]*Dept. of Crop and Soil Sciences, Michigan State University, East Lansing, MI 48824*
[c]*Department of Biological, Chemical and Physical Sciences, Illinois Institute of Technology, Chicago, IL 60616*

Received 11 August 2005
Available online 10 October 2005

Abstract

Biological templating of inorganic nanoparticles provides promising opportunities to address the grand challenge in nanoscience of realizing the full potential of self-assembled materials. We implement such biotemplating to create magnetic nanoparticles by utilizing native protein capsid shells derived in high yield from the T7 bacteriophage virus. The magnetic nanoparticles are grown via bio-mineralization reactions inside of hollowed-out capsids that retain their original chemical recognition properties. The resultant "magnetic viruses" are uniform in geometry, physical properties, and biochemical functionality. We first coax the DNA out of the T7 virus by means of an alkaline treatment, and then grow magnetic cobalt particles inside the remaining hollow capsid shell. Related methods of fabricating bio-functional magnetic nanoparticles have utilized either recombinant, single-protein-type capsids, or involve coating previously synthesized inorganic particles with bio-ligands. Given the richness of the protein types that form the native T7 capsid, our magnetic viruses can be tailored to tune the bio-functionality and/or bio-tagging of a sample. As an example, we consider a nano-biomagnetic sensing scheme that would utilize the T7 capsid to control the magnetic nanoparticle size distribution.
© 2005 Elsevier B.V. All rights reserved.

Keywords: Magnetic nanoparticles; Biomagnetic sensing; Brownian relaxation

Biological architectures have recently attracted much attention as a spatially defined template for fabricating mono-dispersed nanoparticles. It is exciting to explore the possibilities that bio-templating approaches offer in order to specifically create a rich variety of well-defined magnetic nanostructures with interesting properties and functionalities. For example, the apo form of the ferritin protein has been used as a template to fabricate magnetic particles at the nanometer scale [1–2]. In general, biotemplating has included the utilization of bacteria as a host to accommodate the formation of polymer material on the micrometer scale for drug delivery [3], and lipid assemblies, DNA, and multicellular superstructures have been used to direct the patterning and deposition of inorganic material in general in the micro-to-nanometer scale [4–6]. In the present work we utilize a virus-derived template to explore a novel approach to the production of magnetic nanoparticles.

Viruses exemplify an extraordinarily organized nano-architecture which can be harnessed as templates for material synthesis [7–10]. Viruses are complex molecular biosystems in which nucleic acid strands are confined within a nano-sized (~10–500 nm) compartment (capsid) [11–12]. The function of the capsid is to provide a rigid and robust container protecting the nucleic acids in the passage from one host cell to another and to deliver the nucleic acid to the appropriate site. Thus, capsid proteins often have the capacity to be self-assembled into hollow cages in vitro.

☆ The submitted manuscript has been created by the University of Chicago as Operator of Argonne National Laboratory ("Argonne") under Contract no. W-31-109-ENG-38 with the US Department of Energy. The US Government retains for itself, and others acting on its behalf, a paid-up, nonexclusive, irrevocable worldwide license in said article to reproduce, prepare derivative works, distribute copies to the public, and perform publicly and display publicly, by or on behalf of the Government.

*Corresponding authors. Tel.: +1 630 252 4960; fax: +1 630 252 5219.
E-mail addresses: bader@anl.gov (S.D. Bader), lhchen@anl.gov (L. Chen).

0304-8853/$ - see front matter © 2005 Elsevier B.V. All rights reserved.
doi:10.1016/j.jmmm.2005.08.027

Indeed, in vitro self-assembled protein cages derived from plant viruses have been used as containers to host inorganic, including magnetic, oxide mineralization in pioneering work that highlighted the rich opportunities that lie ahead for viral templating [13–16].

T7 bacteriophage particles are especially well suited to be used as templates for inorganic nanoparticles. While many viruses build their capsids and encapsulate their nucleic acids either by co-condensation or by condensing the nucleic acid first and subsequently building a protein shell around it, some viruses, such as tailed T7 phage (a fast growing and extremely stable double-strand DNA phage), build their protein shells first and subsequently condense the nucleic acids within them [17]. As a result, an empty T7 capsid (''ghost virus'') is stable without interior DNA. This is confirmed by the fact that ghost T7 particles are always present in bacterial cultures infected with T7 phage. The outer diameter of the T7 phage is ~55 nm; thus, a T7 ghost can provide a cavity of ~40 nm in the absence of its DNA, which can serve as a template for fabrication of nano-sized particles.

Furthermore, the biological functionality of T7 phage can be readily tailored by generating affinity reagents through phage display technology [18–20]. In phage display, molecules such as antibody fragments, cDNA encoded segments, or combinatorial peptides are expressed as fusions to a capsid protein present on the surface of viral particles. Libraries of millions to billions of phage particles, each displaying a different fusion protein, are screened (usually by affinity selection) for members displaying the desired properties or binding affinities. Phage display offers the following advantages: (a) the peptide or proteins which are expressed on the surface of the viral particles are accessible for interactions with their targets, (b) the recombinant viral particles are highly stable, (c) the viruses can be amplified (grown), and (d) each viral particle contains the DNA encoding its recombinant genome, thereby providing a physical linkage between the genotype and phenotype. Thus, phage libraries can be methodically screened by isolating viral particles that bind to targets, plaque-purifying the recovered phage, and sequencing the phage DNA inserts. Usually three rounds of affinity selection are sufficient to isolate tightly binding phage. Virtually any affinity reagent specific to any target can be displayed on a T7 phage surface via phage display. In our study, we utilized both wild type as well as S-tag peptide, a short peptide with nanomolar affinity to a fragment of RNAse A [21], displayed T7 phage.

Compared to previous work, the significance of using a T7 ghost as a template for magnetic nanoparticle synthesis is two-fold: (i) Because of the morphogenesis of T7, we can use a *native* virus capsid shell, instead of a recombinant capsid shell assembled in vitro from a single type capsid protein. Not only is the native capsid more robust due to the existence of all of its capsid components, but it also can be produced in large quantities. Artificial capsid templates reported on previously were assembled using a recombinant protein. In general, it is very difficult to produce recombinant proteins in high yield. And even if the yields were high, the cost associated with protein purification and production would become prohibitive. In our case, the capsids can be readily obtained directly from the virus. T7 phage can be massively cultured in *Escherichia coli* at low cost, thus our approach offers a practical use of virus capsids as templates for material synthesis. (ii) Because of the establishment of T7 phage display, molecular biology approaches can be engaged to integrate an affinity reagent to the template against virtually any targets via phage display, while maintaining the integration of the virus capsid shell. More importantly, the density (or the number) of the affinity reagent on each template can be precisely controlled. To anchor an affinity reagent to an artificial capsid, one has to generate the affinity reagent first, then link the affinity reagent to the capsid either via chemical conjugation or recombinant fusion, both of which may affect the protein assembling ability, thus altering the assembled capsid's structure. In addition, precise control of the affinity reagent density is very difficulty. Again, our approach provides a practical way of generating a functional virus capsid template, which can lead to uniform functional nanoparticles.

The first goal towards the synthesis of the magnetic viruses is to prepare ghost T7. Previously, ghost T7 capsids have been obtained by normal release from host cells (very low yield) or by osmotic shock [22], which had a reasonably high yield of as high as 55%. In this work, we improved the procedure for preparing T7 ghosts and obtained yields as high as $>98\%$. This was achieved by treating the purified T7 phage with an alkali buffer: the strong alkali condition denatures the capsid proteins and the DNA, permitting the DNA strand to escape. Followed by PEG precipitation of the phage, the capsid proteins are renatured, stable ghost particles form, and ghosts are collected by ultracentrifugation.

The high yield of T7 ghost particles was confirmed by transmission electron microscopy (TEM). As shown in Fig. 1, ghost particles dominate the image. In contrast to the normal T7 (left inset), which have regular icosahedral heads (56 nm in diameter) and short tails (~8 nm), the ghost T7 particles lose their symmetric nature, and are slightly shrunk with an average diameter of 48 nm. Both the normal and ghost T7 phage were negatively stained with uranyl acetate (1%) before TEM imaging. Since uranyl acetate can diffuse inside the capsid, ghost particles have dark core contrast (Fig. 1, and right inset), while the high packing density of DNA inside a normal T7 particle blocks the uranyl acetate uptake into the virus core of the intact viruses. Hence, the normal T7 phage particle has brighter core contrast.

The next goal is to use the ghost virus as a template to grow metallic Co inside the particle instead of the original DNA. This was achieved by utilizing the chemistry of reducing cobalt ions (II) with sodium borohydride [23]. In brief, ghost T7 particles (0.4 mg/ml) were incubated with

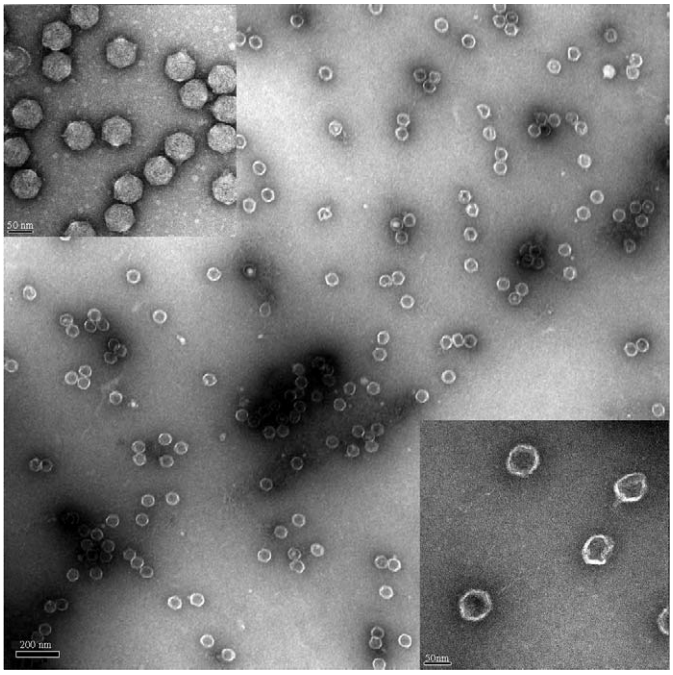

Fig. 1. TEM image of uranyl acetate negatively stained T7 ghost particles after osmotic shock (scale bar = 200 nm). Up–left inset: normal phage particles at higher magnification (scale bar = 50 nm); low–right inset: ghost phage particles (scale bar = 50 nm).

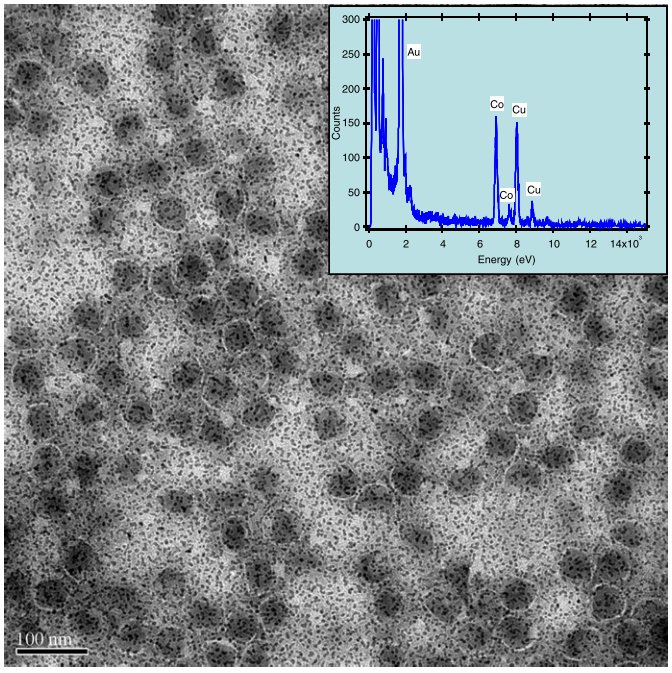

Fig. 2. TEM image of cobalt chimeric T7 phages without negative staining (scale bar = 100 nm). The small particles (1–2 nm) in the background come from the gold particles used for anchoring the chimeric phage; inset: EDX spectrum of the cobalt chimeric T7 phages.

cobalt ions (II) in a degassed, buffered solution at room temperature. After a 1-h incubation, 10 mM $NaBH_4$ was added to the ghost T7-Co (II) mixture under N_2 over a 2-h period. A color change (pink to gray) indicated the formation of cobalt particles. Aside from using Co (II) ions, we conducted a control experiment with hexanitrocobaltate anions, which also can be reduced with $NaBH_4$ to form cobalt metal. However, the yield of magnetic cobalt viruses with hexanitrocobaltate is much lower compared to cobalt (II), which suggests that the negatively charged capsid proteins of the T7 ghost [22] may play a role in attracting the positive cobalt ions, and suggests that positive metal ions are preferred for the formation of chimeric phage.

In order to purify the cobalt particles within the T7 capsid from that formed outside the capsid, we took advantage of the protein coating of the magnetic phage. Thus, amino groups are exhibited outside the magnetic phage, while the free cobalt particles lack such amino groups. By using succinimidyl 3-(2-pyridyldithio) propionate (SPDP) cross-linker, we selectively anchored the magnetic phages onto the surface of a substrate via amide bonds and washed away the cobalt particles formed outside the T7 capsid. Accordingly, we used a gold-coated TEM grid as the substrate to anchor the magnetic phage. After washing off unbound cobalt particles, we were able to image the magnetic phages via TEM. Such an "in vivo" sample preparation process is required to visualize the magnetic phage. Otherwise, the additional cobalt particles (outside the capsid) would induce strong background noise that would make obtaining a clear image impossible. That is why a signal from the gold particles, which were used to anchor the magnetic phage, is present in Fig. 2. However, this does not affect the image quality of the magnetic phage, nor does it interfere with the interpretation. In the future, we could detach the magnetic phage from the substrate after purification. We are working on making a photo-cleavable cross-linker in our lab. With such a cross-linker to anchor the magnetic phage, we will be able to release the magnetic phages from the substrate after the washing steps.

To visualize the magnetic viruses, samples immobilized on a gold-coated TEM grid were imaged by TEM, as shown in Fig. 2. Uniform cobalt particles (42 ± 2 nm) were formed inside the ghost T7. This is supported by energy-dispersive X-ray (EDX) analysis (Fig. 2, inset), where the dominant element inside the T7 ghost is confirmed to be cobalt. The small particles (1–2 nm) in the background come from the gold particles used for anchoring the magnetic viruses.

The next challenge is to determine if the bio-recognition capability of the capsid was preserved. To do this we prepared Co viruses from wild-type and S-tag peptide-displayed T7 phage particles. The S-tag peptide was genetically fused to the capsid protein using T7 Select vector-415-1 (from Novagen). Each S-tag peptide-displayed T7 phage has 415 copies of a 15 amino acid (aa) S-tag displayed on its capsid and the S-tag peptide can interact with 104 aa S-proteins derived from pancreatic ribonuclease A with a 10 nanomolar dissociation constant

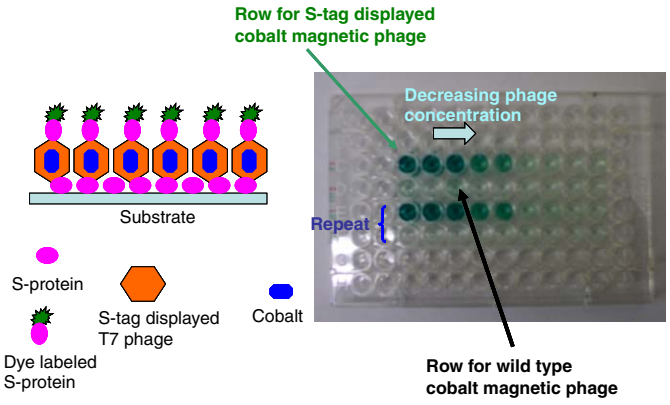

Fig. 3. Left: cartoon for enzyme-linked assay; right: ELISA result for the cobalt chimeric T7 phage.

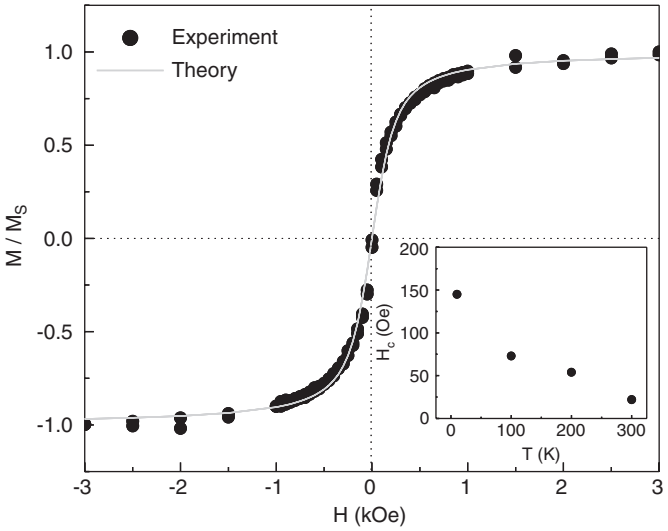

Fig. 4. Magnetization vs. applied magnetic field for cobalt phage in liquid solution. The solid line shows a fit to Eq. (1). The inset shows the temperature dependence of the coercivity for immobilized cobalt phage.

[20]. In contrast the wild-type magnetic viruses serve as a negative control. The different binding affinity of the wild-type and the S-tag-displayed magnetic viruses was demonstrated using an enzyme-linked assay. As shown in Fig. 3, when cobalt magnetic viruses bearing the S-peptide were added to microtiter plate wells coated with the S-protein, we observed strong binding behavior, whereas wild-type cobalt magnetic viruses did not bind to the S-protein at all due to the lack of ligands on their surface. This behavior is the same as that known for the original viruses. Hence, ligand-displayed magnetic viruses maintain their parent's bio-recognition functionality.

Having achieved the goal of preparation while preserving the bio-recognition functionality, we turn to the question of characterizing the magnetic properties, measuring the room-temperature magnetization curve of cobalt magnetic viruses in liquid solution shows paramagnetic behavior, as indicated by the absence of hysteresis (see Fig. 4). This behavior is due to cobalt phages rotating freely in the liquid. In order to estimate the magnetic moment of each cobalt phage, the magnetization curve can be fitted to the classic model of paramagnetism (Langevin function), which is given by

$$M = M_s\left[\coth\left(\frac{\mu H}{k_B T}\right) - \frac{k_B T}{\mu H}\right], \tag{1}$$

where μ is the magnetic moment of each particle. From this fit the magnetic moment for each cobalt phage is $4.7\times10^4\,\mu_B$, which is significantly smaller than the theoretical value $5.2\times10^6\,\mu_B$ estimated for a spherical single-domain cobalt nanoparticle with 40-nm diameter using the value of the bulk saturation magnetization of cobalt ($M_s = 1440\,\mathrm{emu/cm^3}$) at room temperature. This reduced magnetization could be due either to (i) multiple ferromagnetic domains that would arise from the presence of several weakly coupled randomly oriented grains, or (ii) oxidation or hydration of the cobalt during or after the precipitation process. Below the freezing point of the liquid, the magnetization shows hysteresis with non-zero coercivity, as expected for ferromagnetic particles.

In order to ascertain that an individual cobalt phage is truly ferromagnetic at room temperature, we also measured the magnetic behavior of cobalt-chimeric phage that was immobilized on a gold-coated substrate. Fig. 4 (inset) shows the coercivity as a function of temperature for these immobilized cobalt phages. The coercivity decreases with increasing temperature, but remains non-zero at room temperature indicating that the magnetic viruses are indeed ferromagnetic. Therefore, the paramagnetic response of the phage suspended in the liquid is indeed due to rotational Brownian diffusion of the whole particle.

The future challenge is to utilize the magnetic viruses as a new functional entity, for example in biosensing applications. We have considered a scenario whereby we utilize the frequency response of the magnetic susceptibility. The imaginary part of the magnetic susceptibility χ'' has a peak when the applied frequency is the inverse of the Brownian relaxation time [24,25],

$$\tau_B = \frac{\pi\eta d^3}{2k_B T}, \tag{2}$$

where η is the viscosity of the liquid, and d is the particle's effective hydrodynamic diameter. To date, we have shown that we can detect S-protein attachment to suitable coated magnetic nanoparticles, since the hydrodynamic diameter and hence the relaxation time increases after binding [26]. This substrateless approach allows for easy mix-and-measure sensing, where the analyte is mixed into the solution of ferromagnetic particles without any need for further sample preparation. Initial prototype applications of this approach demonstrate a sensitivity of 0.3 pmol [27]. The magnetic virus, with its sharp size control, is expected to yield sharp resonant peaks in χ'' that make the frequency shift analysis an even more powerful tool. Magnetic susceptibility measurements of the cobalt magnetic viruses

in aqueous solution show a peak in χ'' at $\sim$5 kHz. The estimated hydrodynamic diameter is 70 nm using the dynamic viscosity of water at 280 K. This peak disappears when the solution is cooled to 250 K, since the freezing of the liquid immobilizes the nanoparticles. This implies that the frequency peak at room temperature is due to the rotational diffusive Brownian relaxation of the magnetization, and thus the magnetic viruses are suitable for biosensing applications. In contrast to the previously used magnetic nanoparticles, the availability of almost any affinity reagent through phage display allows a straightforward adaptation of this sensing approach to virtually any target using the magnetic viruses.

The fact that the magnetic virus is ferromagnetic and not superparamagnetic has distinct consequences for a variety of possible biomedical applications. For in vivo applications the ferromagnetism could give rise to agglomerations, which could cause embolisms. However, the finite thickness of the protein capsid reduces the dipolar interactions. We estimate that dipolar interactions between particles are negligible compared to the thermal energies. This is confirmed by the observed peak in χ'' at $\sim$5 kHz, indicative of non-interacting particles. One of the advantages is that, besides the possibility to detect Brownian motion, the permanent magnetic moment enables detection in the absence of applied magnetic fields, reducing any diamagnetic or paramagnetic background contributions. In addition, the blocked magnetic moment permits the application of significant forces and torques to the nanoparticles, such as can be used for actuation. Another property of blocked ferromagnetic particles is the possibility for significant heating upon application of AC-magnetic fields, which is advantageous for hyperthermal treatments [28].

In summary, we created novel magnetic viruses via native T7 capsid templating. For the synthesis we used an alkaline treatment to generate hollow T7 phage that subsequently served as the template for the fabrication of cobalt nanoparticles. We confirmed that the resulting magnetic viruses have a uniform cobalt particle diameter of 42 ± 2 nm. Furthermore the bio-functionality is also uniform with 415 copies of ligand attached to each magnetic virus, which can be manipulated by using different types of phage vectors for the starting material. The native virus capsid templating approach provides a robust way to functionalize magnetic nanoparticles with affinity reagents or to tag them with an affinity reagent. We considered a scheme in which this new system can serve as a biosensor. We foresee that magnetic and bio-functional phage can be assembled precisely using a shaped bio-architecture and bio-recognition force. Thus, aside from biomedical applications, such as biosensing, target reagent delivery, magnetic hyperthermal treatments, and MRI contrast enhancement, we anticipate that native virus templated nanoparticles will be of benefit in creating, controlling and tailoring nanomaterials in general.

Acknowledgments

This work was supported by DARPA (8C67400-110) and the US DOE BES-MS under Contract no. W-31-109-ENG-38. We thank Ms. Yimei Chen and Dr. Xiaozhou Liao from University of Chicago for their help with the TEM imaging and EDX analysis. We also thank Dr. Zhaozhong Han for help in preparing the ghost phage.

References

[1] Q.A. Pankhurst, J. Connolly, S.K. Jones, J. Dobson, J. Phys. D: Appl. 36 (2003) R167.
[2] D. Resnick, K. Gilmore, Y.U. Idzerda, M. Klem, E. Smith, T. Douglas, J. Appl. Phys. 95 (2004) 7127.
[3] V. Huter, M.P. Szostak, J. Gampfer, S. Prethaler, W. Lubitz, J. Control. Release 61 (1999) 51.
[4] S. Mann, J. Mater. Chem. 5 (1995) 935.
[5] D.M. Vriezema, M.C. Aragonès, J.A.A.W. Elemans, J.J.L.M. Cornelissen, A.E. Rowan, R.J.M. Nolte, Chem. Rev. 105 (2005) 1445.
[6] A.P. Alivisatos, K.P. Johnsson, X. Peng, T.E. Wilson, C.J. Loweth, M.P. Bruchez Jr, P.G. Schultz, Nature 382 (1996) 609.
[7] I.L. Ivanovska, P.J. de Pablo, B. Ibarra, G. Sgalari, F.C. MacKintosh, J.L. Carrascosa, C.F. Schmidt, G.J. Wuite, Proc. Natl. Acad. Sci. USA 101 (2004) 7600.
[8] S. Zhang, Nat. Biotechnol. 21 (2003) 1171.
[9] M. Sarikaya, C. Tamerler, A.K. Jen, K. Schulten, F. Baneyx, Nat. Mater. 2 (2003) 577.
[10] C. Mao, D.J. Solis, B.D. Reiss, S.T. Kottmann, R.Y. Sweeney, A. Hayhurst, G. Georgiou, B. Iverson, A.M. Belcher, Science 303 (2004) 213.
[11] W. Chiu, R.M. Burnett, R.L. Garcea, Structural Biology of Viruses, University Press, Oxford, 1997.
[12] F.W. Studier, Science 176 (1972) 367.
[13] T. Douglas, M. Young, Nature 393 (1998) 152.
[14] T. Douglas, M. Allen, M. Young, in: A. Steinbüchel (Ed.), Biopolymers, Wiley, VCH, Weinheim, 2002, pp. 405–426.
[15] M. Allen, D. Willits, J. Mosolf, M. Young, T. Douglas, Adv. Mater. 14 (2002) 1562.
[16] S. Brumfield, D. Willits, L. Tang, J.E. Johnson, T. Douglas, M. Young, J. Gen. Virol. 85 (2004) 1049.
[17] S. Casjens, In Virus Structure and Assembly, Jones and Bartlett, Boston, 1985, p. 75.
[18] D.J. Rodi, L. Makowski, Current Opinion in Biotechnology, vol. 10, 1999, p. 87.
[19] J. Kasanov, G. Pirozzi, A.J. Uveges, B.K. Kay, Chem. Biol. 8 (2001) 231.
[20] B.K. Kay, J. Kasanov, M. Yamabhai, Methods 24 (2001) 240.
[21] R.T. Raines, M. McCormick, T.R. VanOosbree, R.C. Mierendorf, Method. Enzymol. 326 (2000) 362.
[22] C. Liu, Q. Jin, A. Sutton, L. Chen, Bioconjugate Chemistry 16 (2005) 1054.
[23] Y. Kobayashi, M. Horie, M. Konno, B. Rodriguez-Gonzalez, L.M. Liz-Marzan, Phys. Chem. B. 107 (2003) 7420.
[24] P. Debye, Polar Molecules, Chemical Catalog Company, New York, 1929.
[25] M.I. Shliomis, Sov. Phys.-Usp. 17 (1974) 153.
[26] S.H. Chung, A. Hoffmann, S.D. Bader, L. Chen, C. Liu, B. Kay, L. Makowski, Appl. Phys. Lett. 85 (2004) 2971.
[27] A. Prieto Astalan, F. Ahrentorp, C. Johansson, K. Larsson, A. Krozer, Biosens. Bioelectron. 19 (2004) 945.
[28] R. Hergt, W. Andrä, C.G. d'Ambly, I. Hilger, W.A. Kaiser, U. Richter, H.-G. Schmidt, IEEE Trans. Magn. 34 (1998) 3745.